Theoretical Study of the Ionized Electronic Structure of the Octahedral Complex MoF_6

Hiroshi Morita, Hiromi Nakai,[#] Pasquale Tomasello,[†] and Hiroshi Nakatsuji*, [##]

Department of Synthetic Chemistry and Biological Chemistry, Faculty of Engineering, Kyoto University, Sakyo-ku, Kyoto 606-01

†Dipartimento di Fisica, Universita di Catania, 57 Corso Italia, I-95129 Catania, Italy

(Received January 23, 1996)

The SAC (symmetry adapted cluster) and SAC-CI (SAC-configuration interaction) theories were used to calculate the ground and ionized states of MoF_6. Compared with the results of previous theoretical studies, the present SAC-CI results are in good agreement with experimental data. We clearly show the effects of the electron correlation and ligand-polarization functions. In this molecule, the ligand polarization even affects the HF orbitals. These polarization functions make the electron density of the ligands expand toward the central metal, which leads not only to a stabilization of the total energy, but also to a destabilization of the valence orbital energies. These changes can be explained by changes in the one- and two-electron integrals. On the other hand, the correlation effect makes the electron density of the ligands expand outwards. This is an inverse effect of the polarization functions.

The electronic structure of the octahedral MoF_6 molecular complex has been studied by photoelectron spectroscopy (PES)[1] and visible-UV spectroscopy.[2] From a theoretical perspective, Bloor and Sherrod[3] studied the excited and ionized states using an overlapping spheres multiple-scattering Xα (OSMXα) calculation. Gutsev and Levin[4] also studied the ionized states using discrete variational Xα (DVMXα) calculations. However, the calculated ionization energies did not agree well with the experimental values, and the assignments were slightly different from those obtained experimentally. For the MoF_6 complex, Sakai and Miyoshi[5] investigated the adiabatic electron affinity (EA) by the configuration interaction (CI) method with the model potential method, showing the importance of the electron correlations. Thus, through previous experimental and theoretical studies, the electronic properties of MoF_6 are now basically understood. However, a more accurate treatment is desirable for definite assignments of the PES and for clarifying the nature of the individual ionized states.

In this study we investigated the electronic structures in the neutral ground and ionized states of MoF_6 by the symmetry adapted cluster (SAC)[6]/SAC-CI[7] method. The accuracy of the SAC-CI method has been confirmed by application it to many organic and inorganic systems.[8] SAC-CI calculations for such metal complexes as RuO_4,[9] OsO_4,[9] $TiCl_4$,[10] $TiBr_4$,[11] and TiI_4[11] have given reasonable and reliable assignments for their PES, and have clarified the spin-orbit effect on the PES. We also examined the effects of adding the polarization and Rydberg functions, since it has been shown that the polarization d function on the F and f function on Au play important roles in calculations of the EA of AuF_6.[12]

Computational Details

MoF_6 shows a regular octahedron geometry with a metal–fluorine bond length of 1.82 Å, based on experimental data.[13] To determine the effect of adding polarization and Rydberg functions, three different Gaussian basis sets were used in this study.

BS1: Mo (43333/433/43)/[433321/4312/421], Huzinaga[14]
+p(0.081, 0.026), Huzinaga[14]
F (73/7)/[721/61], Huzinaga[14]
+p_{anion}(0.074)[15]
BS2: Mo BS1
F BS1
+$d_{polarization}$(3.559, 0.682), Huzinaga[14]
BS3: Mo BS1
+$S_{Rydberg}$(0.01201, 0.005856)[16]
+$P_{Rydberg}$(0.01104, 0.005455)[16]
F BS2
+$S_{Rydberg}$(0.036)[15]
+$P_{Rydberg}$(0.0029)[15]

For the p orbital of Mo, we contract (433) set into [4312] CGTO, because the primitive coefficients are large for two inner exponents. The BS3 set is common to the calculations of the singlet excited states.[17,18]

The electron correlations in the ground state and ion-

#Present address: Waseda University, Department of Chemistry, School of Science and Engineering, Shinjuku-ku, Tokyo 169.
##Also belongs to the Institute for Fundamental Chemistry, 34-4, Takano-Nishihiraki-cho, Sakyo-ku, Kyoto 606.

ized states are taken into account by the SAC theory,[6] and those in the ionized states by the SAC-CI theory[7] using the program SAC85.[19] The active occupied orbitals in the SAC-CI calculations are the 18 higher MOs determined by Hartree–Fock (HF) calculations, performed using the program HONDO8.[20] The active unoccupied orbitals are the 65, 95, and 127 lower MOs for BS1, BS2, and BS3, respectively. The 1, 43, and 43 higher orbitals, whose energies are larger than 4 au, are neglected in the BS1, BS2, and BS3 calculations, respectively.

SAC-CI calculations were performed in the D_{2h} subset of O_h symmetry. The elements of O_h symmetry are associated with those of D_{2h} symmetry as follows:

$$
\begin{aligned}
a_{1g} &= a_g,\\
a_{2g} &= a_g,\\
e_g &= a_g + a_g,\\
t_{1g} &= b_{1g} + b_{2g} + b_{3g},\\
t_{2g} &= b_{1g} + b_{2g} + b_{3g},\\
a_{1u} &= a_u,\\
a_{2u} &= a_u,\\
e_u &= a_u + a_u,\\
t_{1u} &= b_{1u} + b_{2u} + b_{3u},\\
t_{2u} &= b_{1u} + b_{2u} + b_{3u}.
\end{aligned}
$$

Since the (B_{1g}, B_{2g}, B_{3g}) and (B_{1u}, B_{2u}, B_{3u}) states are degenerate in this case, calculations for the B_{2g}, B_{3g}, B_{2u}, and B_{3u} states were omitted.

In the SAC-CI calculations, all single-excitation operators were included in the linked term, and double-excitation operators were selected by the second-order perturbation method.[21] For the ground state, double-excitation operators with a perturbation energy contribution larger than 4×10^{-5} hartree were included. For the ionized states, a threshold of 1×10^{-9} hartree was used with respect to the three ^2A_g, two $^2B_{1g}$, and three $^2B_{1u}$ Koopmans (KP) states. In the SAC-CI theory, triple and quadruple excitations were included in the unlinked terms as products of the lower excitation operators. In calculations of the ionized states, we refer to the calculations which included only triple-excited configurations and those which included both triple- and quadruple-excited configurations in the unlinked terms as "3-excited" and "3, 4-excited" calculations, respectively. These unlinked terms were selected as described previously.[21] Table 1 shows the dimensions of the SAC-CI calculations for the ground and ionized states of MoF_6. By virtue of the SAC-CI formalism, the dimensions of the calculations are small compared with those for the CI method of comparable accuracy.

Results and Discussion

We consider here the valence ionization of MoF_6. The valence occupied MOs of MoF_6 consist of three kinds of the σ-character orbitals ($7a_{1g}$, $7e_g$, and $7t_{1u}$) and four kinds of π-character orbitals ($2t_{2g}$, $6t_{1u}$, $1t_{2u}$, and $2t_{1g}$). Since the $3t_{2g}$ and $8e_g$ MOs due to the 4d AOs of Mo are unoccupied, the valence orbitals mainly comprise the 2p AOs of F. However, as shown in Fig. 1, the 4d AOs of Mo contribute to the $7e_g$ and $2t_{2g}$ MOs, the 5s AO contributes to the $7a_{1g}$ MOs, and the 5p AOs contribute to the $6t_{1u}$ and $7t_{1u}$ MOs. There is a larger mixing of the AOs of Mo in the $7e_g$ and $2t_{2g}$ MOs than in the $7a_{1g}$, $6t_{1u}$, and $7t_{1u}$ MOs, as will be discussed later in a population analysis. Note that the $2t_{1g}$ and $1t_{2u}$ MOs are completely localized on the fluorine atoms. Although there is considerable mixing between the σ- and π-characters in the $6t_{1u}$ and $7t_{1u}$ MOs, as can be seen in Fig. 1, the difference between these MOs is clear in the singlet excitation.[17,18]

Figure 2 shows the experimental and theoretical ionization energies of MoF_6. In comparison with previous Xα calculations, the present SAC-CI results agree with the experimental data, except for the two upper peaks. The discrepancies from the experimental peaks are less than 0.14 eV for the lower five states, while those for the sixth and seventh peaks are 0.55 and 1.02 eV, respectively. As analyzed below, the larger discrepancies for the two upper peaks may be due to the larger orbital reorganization, the description of which requires a

Table 1. Dimension of the SAC and SAC-CI Calculations of MoF_6

Basis set	State	Symmetry[a]	Dimension	
			After selection	Before selection
BS1	Neutral ground state	$^1A_{1g}$	4027	87643
	Ionized state	$^2A_{1g}$	2735	2763
		$^2B_{1g}$	2508	2592
		$^2B_{1u}$	2675	2677
BS2	Neutral ground state	$^1A_{1g}$	5234	185743
	Ionized state	$^2A_{1g}$	3965	4005
		$^2B_{1g}$	3717	3798
		$^2B_{1u}$	3890	3899
BS3	Neutral ground state	$^1A_{1g}$	5584	332209
	Ionized state	$^2A_{1g}$	5049	5373
		$^2B_{1g}$	4622	5070
		$^2B_{1u}$	4949	5219

a) SAC-CI calculations were performed in the D_{2h} subset of O_h symmetry.

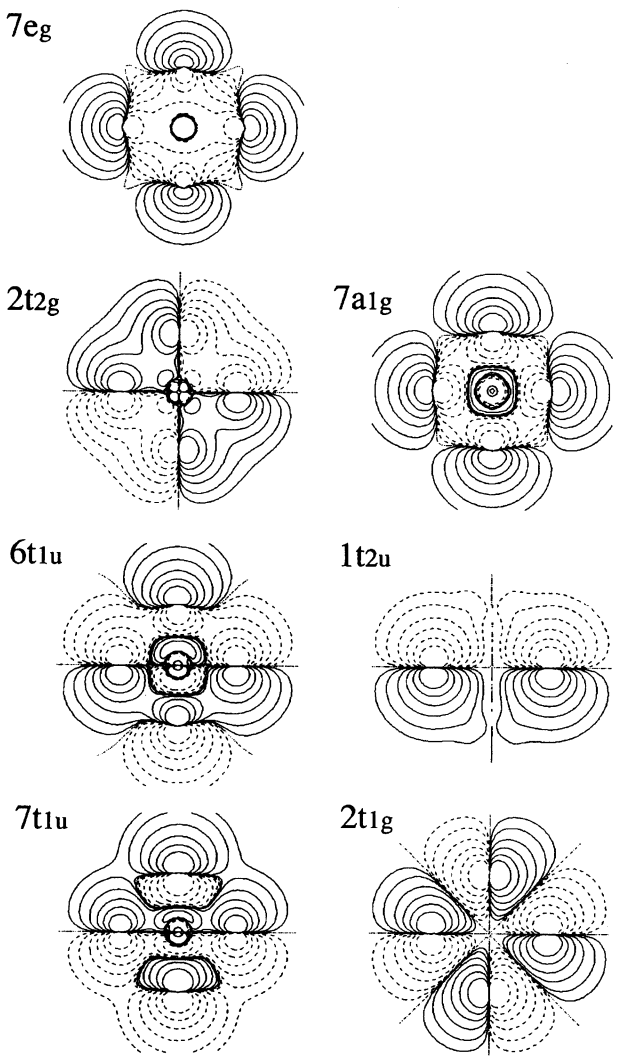

Fig. 1. Contour maps of the valence occupied MOs of MoF_6. Solid and broken lines correspond to plus and minus signs in the MO, respectively. The absolute values of the contours are 0.3, 0.1, 0.03, 0.01, 0.003, and 0.001.

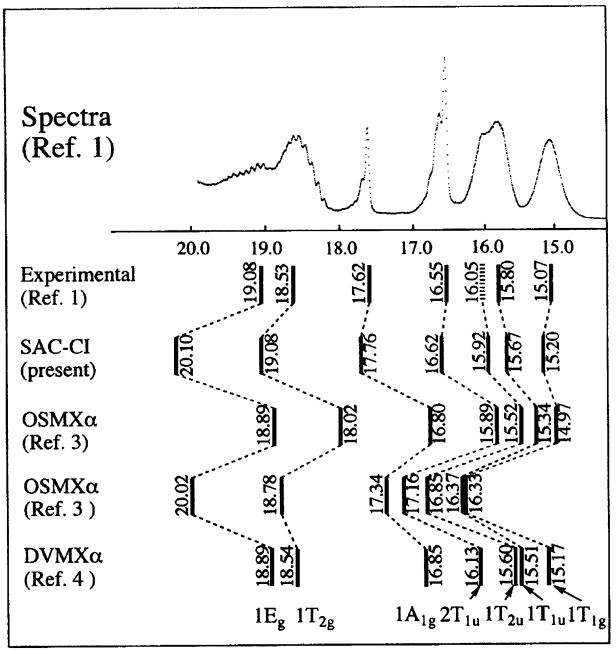

Fig. 2. Comparison of the ionization energies of MoF_6 calculated in the present and previous studies and their assignments for the observed peaks in the PES (Ref. 1). The two OSMXα calculations differ in the parameter of the atomic radius.

higher order of the excitation configurations.

The present assignments (Fig. 2) are the same as those from previous theoretical studies. Karlsson et al. assigned the second strong band at 15.80 eV to ionization from the $7t_{1u}$ MO, and the splitting of this band was thought to reflect Jahn–Teller distortion.[1] On the other hand, the present and previous theoretical studies showed a different ionized state for this splitting; i.e., ionization from the $1t_{2u}$ MO.

We then examined the effects of augmented basis functions, such as the polarization and Rydberg bases, and electron correlations. Figure 3 shows the ionization energies calculated by the KP and SAC-CI methods with three different basis sets. For SAC-CI, both the "3-excited" and "3,4-excited" calculations are shown. Although the ordering of the ionized states in Fig. 3 is the same with each method, the energy levels are shifted lower with the larger basis sets. However, the energy shifts from BS2 to BS3 are much smaller than those from BS1 to BS2 in each case. This means that, compared with the polarization d functions of F, the Rydberg functions of both Mo and F are not important for describing the ionized states of MoF_6.

It is interesting that the polarization functions affect not only the correlated calculations, but also the HF calculations. The KP results indicate that the orbital energies are destabilized by the addition of polarization functions, even though the total energies are stabilized: −4568.944042 au (BS1), −4569.120976 au (BS2), and −4569.125835 au (BS3). In the HF approximation, the orbital and total energies are represented by

$$\varepsilon_i = h_i + \sum_j^N (2J_{ij} - K_{ij}) \tag{1}$$

and

$$E_O = \sum_i^N h_i + \frac{1}{2}\sum_i^N \sum_j^N (2J_{ij} - K_{ij}) = \sum_i^N \varepsilon_i - \frac{1}{2}\sum_i^N \sum_j^N (2J_{ij} - K_{ij}), \tag{2}$$

where N is the total number of electrons, h is the one-electron integral (OEI), and J and K are the Coulomb and exchange integrals, respectively. Table 2 shows the values of the OEI and two-electron integral (TEI) terms for the orbital energies in the BS1 and BS3 calculations. Table 2 also shows the contributions of the kinetic energy (KE) and nuclear attraction (NA) terms for the OEI. Except for the $7e_g$ and $2t_{2g}$ MOs, the shifts in the orbital energies are due to the increase in the TEIs. Despite destabilization of the TEIs, the stabilization of the total energy is mainly due to the OEI, in which the NA term is larger than the KE term.

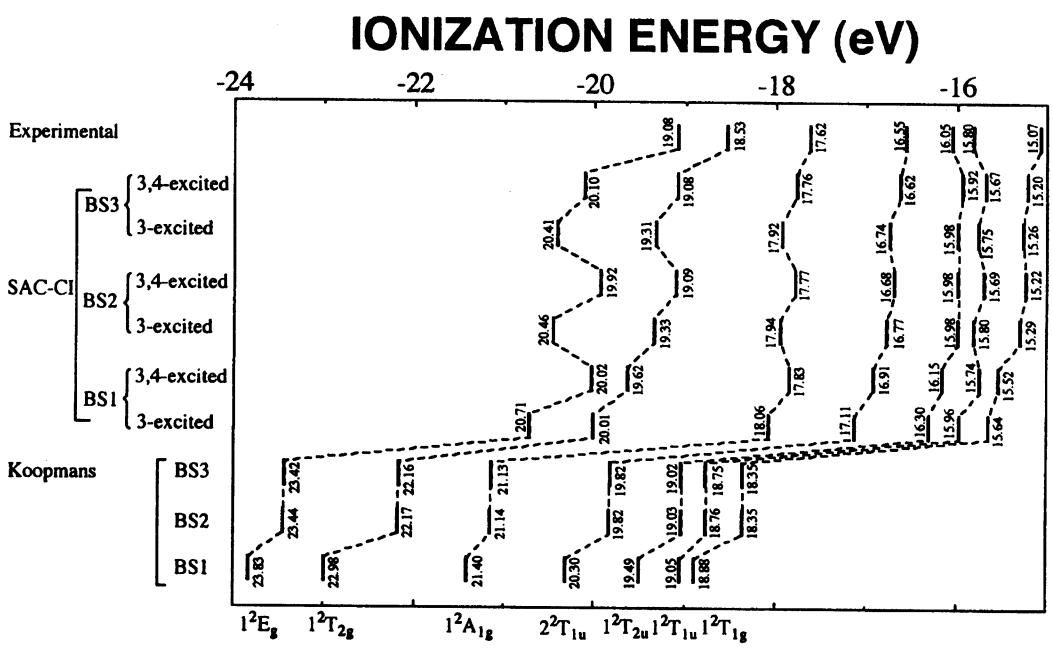

Fig. 3. Comparison of the ionization energies of MoF_6 calculated by the Koopmans and SAC-CI methods with different basis sets. "3-excited" and "3,4-excited" are defined in the text.

Table 2. Comparison of the Orbital Energy and One- and Two-Electron Integrals Between the BS1 and BS3 Calculations

The contributions of the kinetic energy and nuclear attraction terms are shown for the one-electron integral (eV).

Basis set	Orbital	Orbital energy	One-electron integral			Two-electron integral
			Kinetic energy	Nuclear attraction	Total	
BS1	$7e_g$	−23.8285	97.0822	−983.2785	−886.1963	862.3678
	$2t_{2g}$	−22.9836	77.5084	−932.9067	−855.3983	832.4147
	$7a_{1g}$	−21.4005	98.7246	−908.4008	−809.6762	788.2757
	$6t_{1u}$	−20.3029	91.3687	−888.9868	−797.6181	777.3152
	$1t_{2u}$	−19.4913	87.3823	−867.7314	−780.3491	760.8578
	$7t_{1u}$	−19.0502	100.1925	−900.0480	−799.8555	780.8053
	$2t_{1g}$	−18.8813	93.0596	−877.0716	−784.0120	765.1307
BS3	$7e_g$	−23.4214	94.7755	−980.7454	−885.9699	862.5485
	$2t_{2g}$	−22.1600	77.4531	−925.9914	−848.5383	826.3783
	$7a_{1g}$	−21.1316	98.1457	−916.6316	−818.4858	797.3542
	$6t_{1u}$	−19.8194	93.1757	−899.9125	−806.7368	786.9175
	$1t_{2u}$	−19.0187	86.8676	−872.0843	−785.2167	766.1980
	$7t_{1u}$	−18.7537	98.0602	−904.6971	−806.6370	787.8833
	$2t_{1g}$	−18.3457	92.4285	−879.9172	−787.4888	769.1431
Difference (BS3-BS1)	$7e_g$	0.4071	−2.3067	2.5332	0.2264	0.1807
	$2t_{2g}$	0.8237	−0.0552	6.9153	6.8600	−6.0364
	$7a_{1g}$	0.2689	−0.5789	−8.2308	−8.8096	9.0785
	$6t_{1u}$	0.4835	1.8070	−10.9257	−9.1188	9.6023
	$1t_{2u}$	0.4726	−0.5148	−4.3529	−4.8676	5.3403
	$7t_{1u}$	0.2966	−2.1323	−4.6491	−6.7815	7.0780
	$2t_{1g}$	0.5356	−0.6312	−2.8456	−3.4767	4.0124

Figure 4 shows density-difference maps for the valence occupied orbitals in the BS1 and BS3 calculations. The density difference for the i-th MO (ϕ_i) is defined by

$$\Delta\rho(\boldsymbol{r}) = \left|\phi_i^{\mathrm{BS3}}(\boldsymbol{r})\right|^2 - \left|\phi_i^{\mathrm{BS1}}(\boldsymbol{r})\right|^2. \quad (3)$$

As can be seen in Fig. 4, the electron densities of the ligands are polarized toward the central metal. This is a normal effect of the polarization functions; namely,

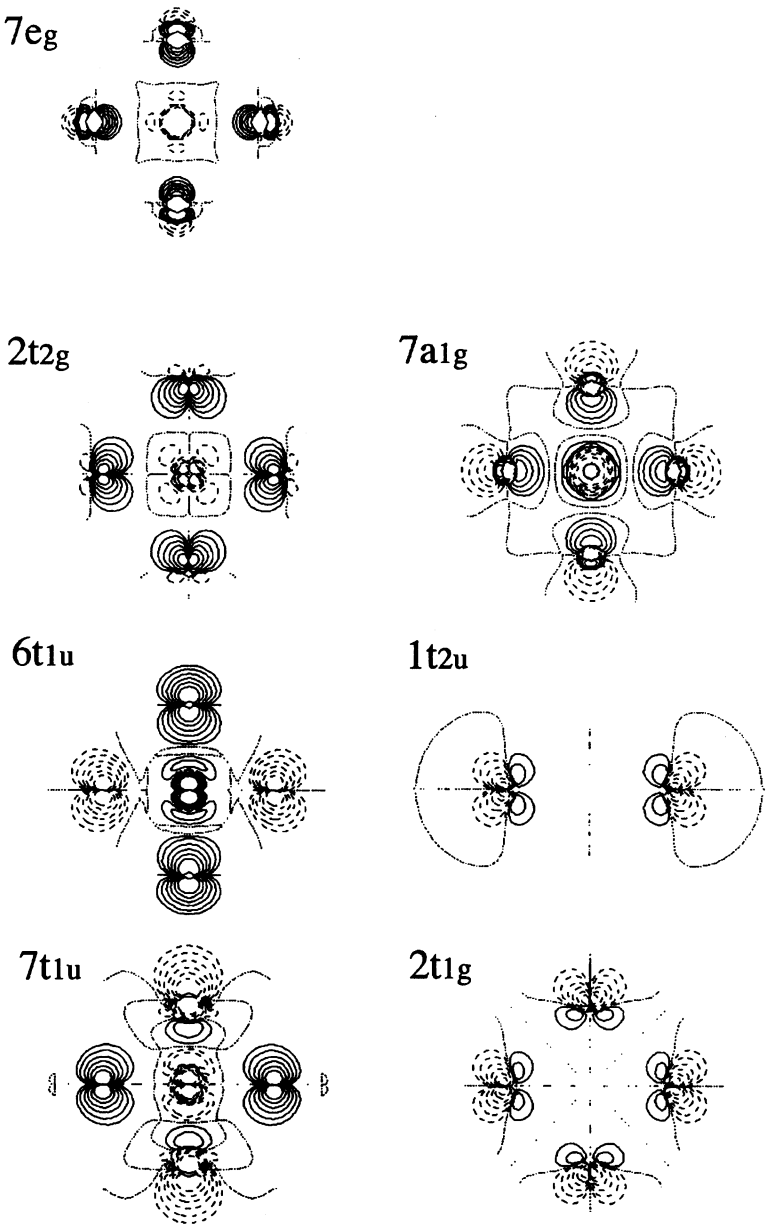

Fig. 4. Contour maps of the density difference of the HF orbitals using BS1 and BS3. Solid and broken lines correspond to plus and minus signs in the density difference, respectively. The absolute values of the contours are 0.3, 0.1, 0.03, 0.01, 0.003, and 0.001.

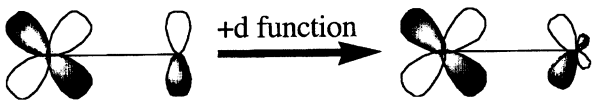

(4)

This polarization seems to induce a larger attraction between the electron density and the nucleus of the central metal. However, the increase in the electron density in the M–L bonding region would produce a larger electron repulsion. These energy changes are given in Table 2. As for the $6t_{1u}$ and $7t_{1u}$ MOs, we can see enhanced mixing between the σ- and π-characters, which leads to an increase in the absolute values of the KE and NA terms for the $6t_{1u}$ MO.

The $2t_{2g}$ and $7e_g$ MOs require a slightly different analysis. In Table 2, the value of the OEI for the $2t_{2g}$ MO is destabilized and that of the TEI is stabilized by addition of the d functions. The $2t_{2g}$ MO provides bonding between the ligands as well as between the metal and the ligands, as shown in Fig. 1. This may produce a polarization of the electron density toward the L–L bonding region, which seems to reduce the NA energy. On the other hand, the reorganization of the electron density in the $7e_g$ MO is quite small. Therefore, the energy changes in the OEI and TEI are small compared with those in the other MOs given in Table 2. It is interesting that the shift in the orbital energy for the $7e_g$ MO is on the same order as those of other MOs.

We next investigated the correlation effects in the ionized states of MoF_6 in more detail. Since the shifts in the ionized energies using the KP method and the SAC-CI method are more than 3.0 eV (Fig. 3), the electron correlations are indis-

pensable for describing the ionized states of MoF_6. Furthermore, including the quadruple-excited configurations moves the energy shifts to lower values. This effect is larger in the 1^2T_{2g} and 1^2E_g states (energy shifts of 0.23 and 0.31 eV, respectively) then in the other states. The importance of the higher excitations means a large relaxation in the ionized states, which should appear in the net charges.

Table 3 gives the net charges of the neutral ground and ionized states calculated by the KP and SAC-CI methods using BS3. The ionicity of the Mo–F bond in the ground and ionized states is lower with the SAC-CI method than with the KP method. In the KP calculations, the net charges of Mo in the 1^2T_{2g} and 1^2E_g states are changed by +0.230 and +0.228 from the neutral state, respectively. These changes are larger than those in other states, which means that the mixing of the orbitals of Mo is larger in the $2t_{2g}$ and $7e_g$ MOs. On the other hand, the net charges of Mo change by only +0.007 and +0.091 in the SAC-CI calculations. Therefore, the relaxations in the 1^2T_{2g} and 1^2E_g states are large.

Finally, we examined the spatial distribution of the relaxation by including the electron correlations. Figure 5 shows the contour maps of the density difference defined by

$$\begin{aligned}\Delta\rho(\boldsymbol{r}) &= \left(\left|\Psi_N^{SAC}(\boldsymbol{r})\right|^2 - \left|\Psi_I^{SAC-CI}(\boldsymbol{r})\right|^2\right) \\ &\quad - \left(\left|\Psi_N^{HF}(\boldsymbol{r})\right|^2 - \left|\Psi_I^{KP}(\boldsymbol{r})\right|^2\right) \\ &= \left(\left|\Psi_N^{SAC}(\boldsymbol{r})\right|^2 - \left|\Psi_I^{SAC-CI}(\boldsymbol{r})\right|^2\right) - \left|\phi_i^{HF}(\boldsymbol{r})\right|^2, \quad (5)\end{aligned}$$

where Ψ is the total wave function in the neutral (N) and ionized (I) states of MoF_6, and the superscripts show the method used. The density difference defined by Eq. 5 indicates the difference in the distribution of the detached electron between the HF (KP) and SAC-CI calculations. The distribution of the detached electron based on HF (KP) calculations corresponds to the HF orbital.

The electron densities on Mo increase in all cases, and the increment is largest in the 1^2T_{2g} and 1^2E_g states, as shown in Table 3. The orbitals responsible for these ionizations have the bonding nature between the F 2p and Mo 4d orbitals, which increases the ionization energies. We speculate that electron relaxation should lead to a decrease in the bonding

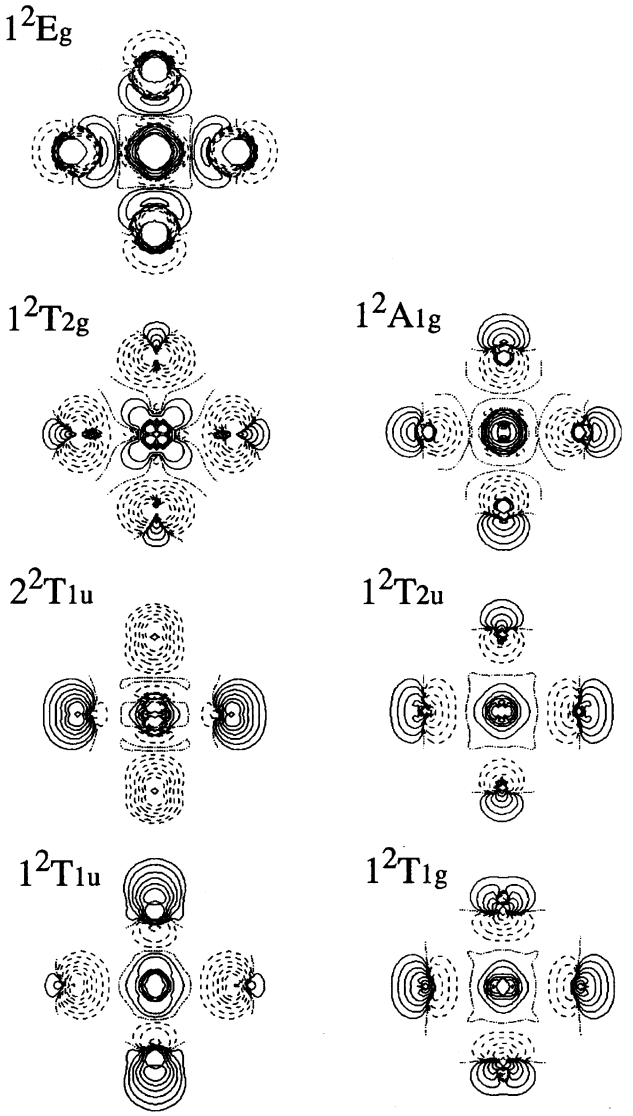

Fig. 5. Contour maps of the density difference of the detached electron using the HF (KP) and SAC-CI methods. Solid and broken lines correspond to plus and minus signs in the density difference, respectively. The absolute values of the contours are 0.3, 0.1, 0.03, 0.01, 0.003, and 0.001.

Table 3. Net Charge in the Neutral Ground and Ionized States of MoF_6 Calculated by the SAC-CI and Koopmans Methods

Ionized	Koopmans		SAC-CI	
state	Mo	F	Mo	F
ground	+1.538	−0.256	+1.226	−0.204
1^2T_{1g}	+1.538 (0.0)	−0.089 (0.167)	+1.323 (0.097)	−0.054 (0.150)
1^2T_{1u}	+1.554 (0.016)	−0.092 (0.164)	+1.335 (0.109)	−0.056 (0.148)
1^2T_{2u}	+1.538 (0.0)	−0.089 (0.167)	+1.246 (0.020)	−0.041 (0.163)
2^2T_{1u}	+1.620 (0.082)	−0.103 (0.153)	+1.235 (0.009)	−0.039 (0.165)
1^2A_{1g}	+1.621 (0.083)	−0.103 (0.153)	+1.304 (0.078)	−0.051 (0.153)
1^2T_{2g}	+1.768 (0.230)	−0.128 (0.128)	+1.233 (0.007)	−0.039 (0.165)
1^2E_g	+1.766 (0.228)	−0.127 (0.129)	+1.317 (0.091)	−0.053 (0.151)

a) Values in parentheses show the difference from the ground.

nature.

In the 1^2T_{1g}, 1^2T_{2u}, and 1^2A_{1g} states, the electron densities of the ligands expand outward. The electron correlations may lead to scattering of the electrons from the bonding regions to the outer regions. The changes in the 1^2T_{1u} and 2^2T_{1u} states emphasize the σ- and π-characters of the $7t_{1u}$ and $6t_{1u}$ MOs, respectively. Note that the behaviors of the electron density differences in Fig. 5 are opposite to those in Fig. 4.

Concluding Remarks

We used the SAC-CI method to calculate the ground and ionized states of MoF_6. The calculated ionization energies compare well with experimental results, except for the two upper bands. The present assignments are the same as previous theoretical assignments, whereas they differ slightly from experimental assignments. Specifically, we consider the peaks at 15.80 and 16.05 eV to be ionized states from the $7t_{1u}$ and $1t_{2u}$ orbitals, while an experimental study suggested that these were due to a Jahn–Teller splitting.

We also examined the effects of the electron correlation and ligand polarization functions. The polarization functions of the ligands influence even the HF orbitals. Destabilization of the orbital energies is due to an increase in the two-electron repulsion, whereas stabilization of the total energy is caused by one-electron integrals, especially by the nuclear attraction terms. These conclusions can be clearly demonstrated using the electron-density difference.

An analysis of the net charges and density difference maps shows larger relaxations in the two upper states, 1^2T_{2g} and 1^2E_g. In conclusion, the higher order of the excitation configurations is essential for a reliable description of these two states. It is suitable for this case to use the SAC-CI (general-*R*) method,[22] which includes the higher excitation operater in the linked operater. However, the main configurations of these states are one-electron ionizations from the $2t_{2g}$ and $7e_g$ MOs.

The calculations were carried out using computers in our laboratory and at the Computer Center of the Institute for Molecular Science. This study was supported in part by a Grant-in-Aid for Scientific Research from the Ministry of Education, Science, and Culture of Japan and by the New Energy and Industrial Technology Development Organization (NEDO).

References

1) L. Karlsson, L. Mattsson, R. Jafrny, T. Bergmark, and K. Siegbahn, *Phys. Scr.*, **14**, 230 (1976).
2) R. McDiarmid, *J. Chem. Phys.*, **61**, 3333 (1974).
3) J. E. Bloor and R. E. Sherrod, *J. Am. Chem. Soc.*, **102**, 4333 (1980).
4) G. L. Gutsev and A. A. Levin, *Chem. Phys.*, **51**, 459 (1980).
5) Y. Sakai and E. Miyoshi, *J. Chem. Phys.*, **87**, 2885 (1987); E. Miyoshi, Y. Sakai, A. Murakami, H. Iwaki, H. Terashima, T. Shoda, and T. Kawaguchi, *J. Chem. Phys.*, **89**, 4193 (1988).
6) H. Nakatsuji and K. Hirao, *J. Chem. Phys.*, **68**, 2035 (1978).
7) H. Nakatsuji, *Chem. Phys. Lett.*, **59**, 362 (1978); **67**, 329 and 334 (1979).
8) H. Nakatsuji, *Acta Chim. Hung.*, **129**, 719 (1992).
9) H. Nakatsuji and S. Saito, *Int. J. Quant. Chem.*, **39**, 93 (1991).
10) H. Nakatsuji, M. Ehara, M. H. Palmer, and M. F. Guest, *J. Chem. Phys.*, **97**, 2561 (1992).
11) H. Nakatsuji and M. Ehara, *J. Chem. Phys.*, **101**, 7658 (1994).
12) E. Miyoshi and Y. Sakai, *J. Chem. Phys.*, **89**, 7363 (1988).
13) H. M. Seip and R. Seip, *Acta Chem. Scand.*, **20**, 2698 (1966).
14) S. Huzinaga, J. Andzelm, M. Klobukowski, E. Radzio-Andzelm, Y. Sakai, and H. Tatewaki, "Gaussian Basis Sets for Molecular Calculations," Elsevier, New York (1984).
15) T. H. Dunning, Jr., and P. J. Hay, "Modern Theoretical Chemistry," ed by H. F. Schaeffer, III, Plenum, New York (1977), Vol. 3.
16) M. Jungen, *J. Chem. Phys.*, **74**, 750 (1981).
17) H. Nakai, H. Morita, and H. Nakatsuji, *J. Phys. Chem.*, in press.
18) H. Nakai, H. Morita, P. Tomasello, and H. Nakatsuji, unpublished.
19) H. Nakatsuji, Program System for SAC and SAC-CI Calculations, Program Library No. 146 (Y4/SAC), Data Processing Center of Kyoto University, (1985); Program Library SAC85, No. 1396, Computer Center of the Institute for Molecular Science, (1986).
20) M. Dupuis and A. Farazdel, Program System HONDO8 from MOTECC-91 (1991).
21) H. Nakatsuji, *Chem. Phys.*, **75**, 425 (1983).
22) H. Nakatsuji, *Chem. Phys. Lett.*, **177**, 331 (1991).